



Evaluation of alumina nanoparticles concentration and stirring rate on wear and corrosion behavior of nanocomposite PEO coating on AZ31 magnesium alloy



M. Asgari, M. Aliofkhazraei*, Gh. Barati Darband, A. Sabour Rouhaghdam

Department of Materials Engineering, Faculty of Engineering, Tarbiat Modares University, P.O. Box: 14115-143, Tehran, Iran

ARTICLE INFO

Article history:

Received 17 July 2016

Revised 19 October 2016

Accepted in revised form 14 November 2016

Available online 16 November 2016

Keywords:

Stirring rate

Magnesium

Alumina nanoparticles

Corrosion resistance

Wear resistance

ABSTRACT

The effect of electrolyte stirring rate and concentration of nanoparticles on alumina nanoparticles absorption in the coating fabricated by plasma electrolytic oxidation on magnesium substrate was investigated. Microstructure, corrosion resistance and wear behavior of the nanocomposite coating were analyzed by scanning electron microscopy (SEM), potentiodynamic polarization and electrochemical impedance spectroscopy, and pin-on-disk tests, respectively. The results showed that the highest amount of nanoparticle absorption happened at the stirring rate of 100 rpm, and decreased at higher stirring rates because of the high turbulence of the electrolyte, which washes the nanoparticles away from the surface of the anode. The effect of alumina concentration in the electrolyte on the alumina nanoparticles' absorption was also analyzed, and the results indicated that by increasing the concentration of nanoparticles in the electrolyte, the absorption of nanoparticles increased up to 30 g/L, and then reached the saturated level. Also the best corrosion resistance the lowest wear rate was obtained in the stirring rate of 100 rpm at a concentration of 30 g/L of alumina nanoparticles.

© 2016 Elsevier B.V. All rights reserved.

1. Introduction

Due to the high strength to weight of magnesium alloys, they have high potential to be used in the industrial applications [1]. However, magnesium is one of the most active metals due to its low standard potential. So magnesium and its alloys have poor corrosion resistance, which leads to limitations in their use in corrosive environments [2,3]. Magnesium and its alloys are extremely susceptible to galvanic corrosion that decreases their mechanical stability and thus creates unpleasant appearance. With regard to magnesium's working conditions, surface processes are essential for its alloys [4]. So far, various methods of coating have been studied to protect magnesium against corrosion; they include electrochemical plating, PVD and CVD, conversion coating anodizing and polymer coatings. Among them, conversion and anodizing coatings are the most common [5]. Anodizing is a relatively simple and inexpensive method but the coatings fabricated in this way are thin and porous and cannot provide the required corrosion resistance in corrosive environments [6–8].

Parallel to various efforts to create advanced anodizing processes in the '70s and '80s in the Union of Soviet Socialist Republics (USSR), the possibility of fabricating oxide on different metal surfaces is analyzed by surface electrical discharges [9]. Due to the relatively new process of PEO and its high potential to create high-quality coatings and highly

desirable properties, the need to do research on it is strongly recommended [10].

Plasma electrolytic oxidation (PEO) is based on anodic polarization in an electrolyte solution under plasma discharge conditions on the anode surface [11]. This process can be used for metals such as aluminum, titanium, magnesium and their alloys (valve metal). There is a high tendency to use these coatings due to the high rate of the process, being economically affordable, and possible using for components in any form or size. The process products may be quite dense and hard [12]. An important feature of these coatings is that the hard oxide layer grows inward on the substrate surface; therefore, it is possible to achieve coatings with good adhesion and dimensional stability on the surface of the substrate. Unlike the super-hard coatings, it is possible to obtain coatings with a thickness over 100 μm in this approach. These features expand the usage of these coatings in different applications such as abrasion resistance, wear resistance, corrosion resistance, electrical insulation, thermal protection, etc. [13].

Nanocomposite coatings have at least two different phases in their structure; one of them is in nano scale. They can be obtained by plasma electrolytic oxidation process. Among the nano composite coatings include plasma electrolytic oxidation coatings with nanoparticles [14–16]. The use of nanoparticles improves the physical and mechanical properties of the coatings. Several researchers have reported the increase in corrosion resistance and wear in coatings with alumina nanoparticles [17–19]. The optimum concentration of nanoparticles is among the important factors in these types of coatings. Of course,

* Corresponding author.

E-mail addresses: maliofkh@gmail.com, khazraei@modares.ac.ir (M. Aliofkhazraei).

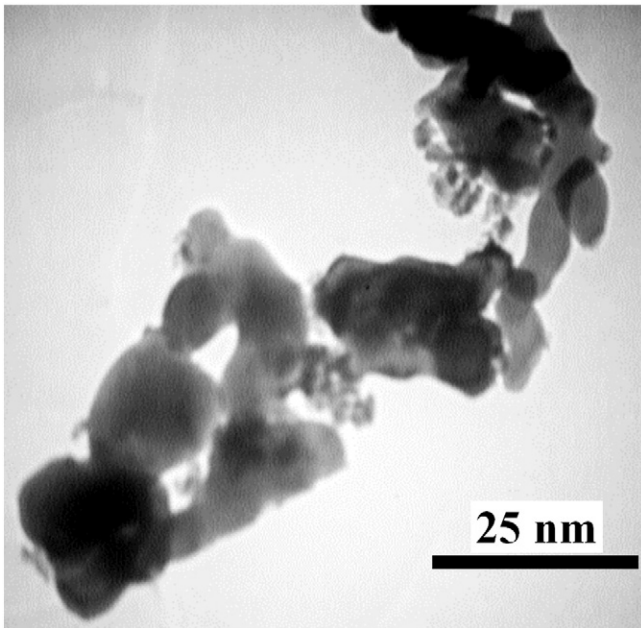


Fig. 1. TEM image of alumina nanoparticles.

coating parameters can affect the optimum concentration and absorption of nanoparticles. Many parameters are effective in plasma electrolytic oxidation process. It can be stated that almost all parameters influencing the chemical electrolysis processes, are important in the PEO process. Basically, the properties of the fabricated coatings by this method are affected by the substrate, alloying elements, type of source power, applied current density, anode voltage range, electrolyte composition and concentration, electrolyte temperature, the distance between anode and cathode, electrolyte stirring rate, etc. [20]. The most important parameter affecting the coating properties is the absorption of nanoparticles, and the main factors effective in the absorption of nanoparticles are electrolyte stirring rate and type of stirring in the electrolyte [21]. There are a variety of ways to create flow and turbulence in the electrolyte; one of them is the use of magnetic stirrers [22,23].

Based on our knowledge, the effect of stirring rate on nanoparticle absorption in the PEO coating has not been investigated yet, therefore, in this study, the effect of electrolyte stirring rate by magnetic stirrers

and the concentration of nanoparticle, on their absorption, and consequently, microstructure, corrosion resistance and wear resistance of the fabricated coating are investigated.

2. Experimental

In this study, oxide layers were created on AZ31B magnesium alloy by PEO method. Sample preparation was done by sanding and degreasing. For this purpose, the rough-to-soft- sanding papers were used, and alcohol solution (96%) was employed for degreasing. For coating treatment, the direct current DC and rectangular stainless steel-304 cathode with the dimensions 50×80 mm were used. To perform the process, simply dilute alkaline solutions with different concentrations alumina nanoparticles were employed. The TEM image of alumina nanoparticles is shown in Fig. 1. The approximate composition of the electrolyte used in the experiments includes sodium phosphate ($\text{Na}_3\text{PO}_4 \cdot 12\text{H}_2\text{O}$) (5 g/L) and potassium hydroxide (KOH) (2 g/L). PH of the solutions was measured as 12–12.5, and in performing the process, the heater stirrer was used to smooth the solution; one of the studied variables was the stirring rate that varied between 50, 100, 300, 500 and 700. Another important parameter was the optimization of the alumina nanoparticles added to the solution at the concentrations of 10, 20, 30 and 40 g/L. For dispersing the nanoparticles in the electrolyte, they were added to the deionized water and dispersed on the stirrer for 24 h; then they were dispersed ultrasonically for 1 h. The coatings microstructure was studied by the scanning electron microscopy (SEM); and the corrosion resistance of the layers was analyzed in the conventional solution of sodium chloride 3.5 wt% (pH = 7.6, exposure time = 15 min) using potentiodynamic polarization and electrochemical impedance spectroscopy (EIS) tests. The EG & G device (model A273) was used for electrochemical analysis. Then the test was performed in standard electrochemical cell on the three-electrode mode in which platinum was used as the counter electrode, saturated calomel was the reference electrode, and the coated substrate was used as the working electrode. The potentiodynamic polarization test was performed with a scan rate of 1 mV at 0.2 V lower than OCP to 0.8 above it. EIS test was done in the frequency range of 65 kHz to 0.01 Hz at a frequency of 10 mV and in open-circuit potential. Pin-on-disk test was carried out to investigate the wear behavior of the coatings. The employed pin was made of a polymer material, called POLYBON, and the applied force and velocity were 45 N and 100 rpm respectively. The travelled distance for all specimens was the same equal to 200 m.

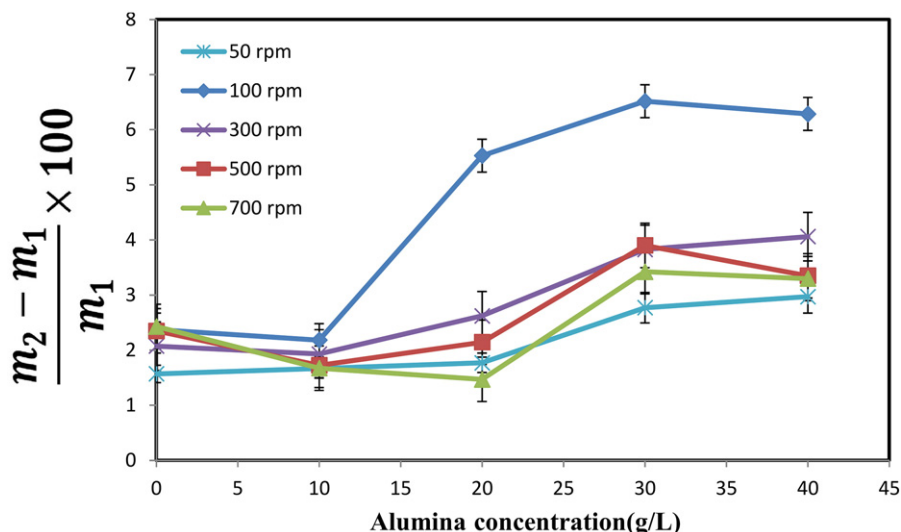


Fig. 2. Effect of alumina nanoparticles concentration in the electrolyte and stirring rate on the adsorption of nanoparticles.

3. Results and discussion

3.1. Nanoparticle absorption

Various factors affect the absorption of nanoparticles inside the coating including the concentration of nanoparticles in the electrolyte, as well as the stirring rate. Since nanoparticles are of oxide type, they are not ionized inside the electrolyte. Thus their absorption in the coating cannot be due to the electrochemical reactions. Researchers believe that absorption of nanoparticles in the coating is mostly due to the electrophoretic and mechanical forces of the electrolyte stirring rate [24–27]. Accordingly, entering of the particles into the PEO coating area adjacent to the anode requires an outside force to transfer the nanoparticles toward the interface of coating/electrolyte. After the distribution of the particles in the electrolyte and combination with the hydroxide ions, the particles are negatively charged, and due to strong electric field between the anode and the cathode, they are sent to the anode side, and during the process, they are absorbed inside the coating structure [11]. Thus, it can be concluded that the electrolyte stirring rate

affects the absorption of nanoparticles in the coating. Also creation of discharges during the coating process [28] as well as electrolyte evaporation due to the high temperature of the micro dischargers [29] are effective in the absorption of nanoparticles in the coating. Furthermore, according to Aliofkhaezai et al. [30], factors such as agglomeration of nanoparticles in the pores, coating density, and eruption of molten oxide from the substrate to the surface of the coating can be the main obstacles to the entering of nanoparticles into the coatings. The effect of alumina nanoparticles concentration in the electrolyte and stirring rate on the adsorption of nanoparticles is shown in Fig. 2. Since the other variables such as concentration of other electrolyte components have been considered fixed in this study, thus the changes in the coatings weight are caused by the changes in the nanoparticles' absorption; higher changes in weight indicate higher nanoparticle absorption. In this study, six different concentrations (between 0 and 40 g/L) of alumina nanoparticles as well as five stirring rates (50, 100, 300, 500 and 700 rpm) have been used. The first effect that can be explored is the effect of nanoparticles concentration in the electrolyte on their absorption. As shown in Fig. 2, by increasing the concentration of alumina

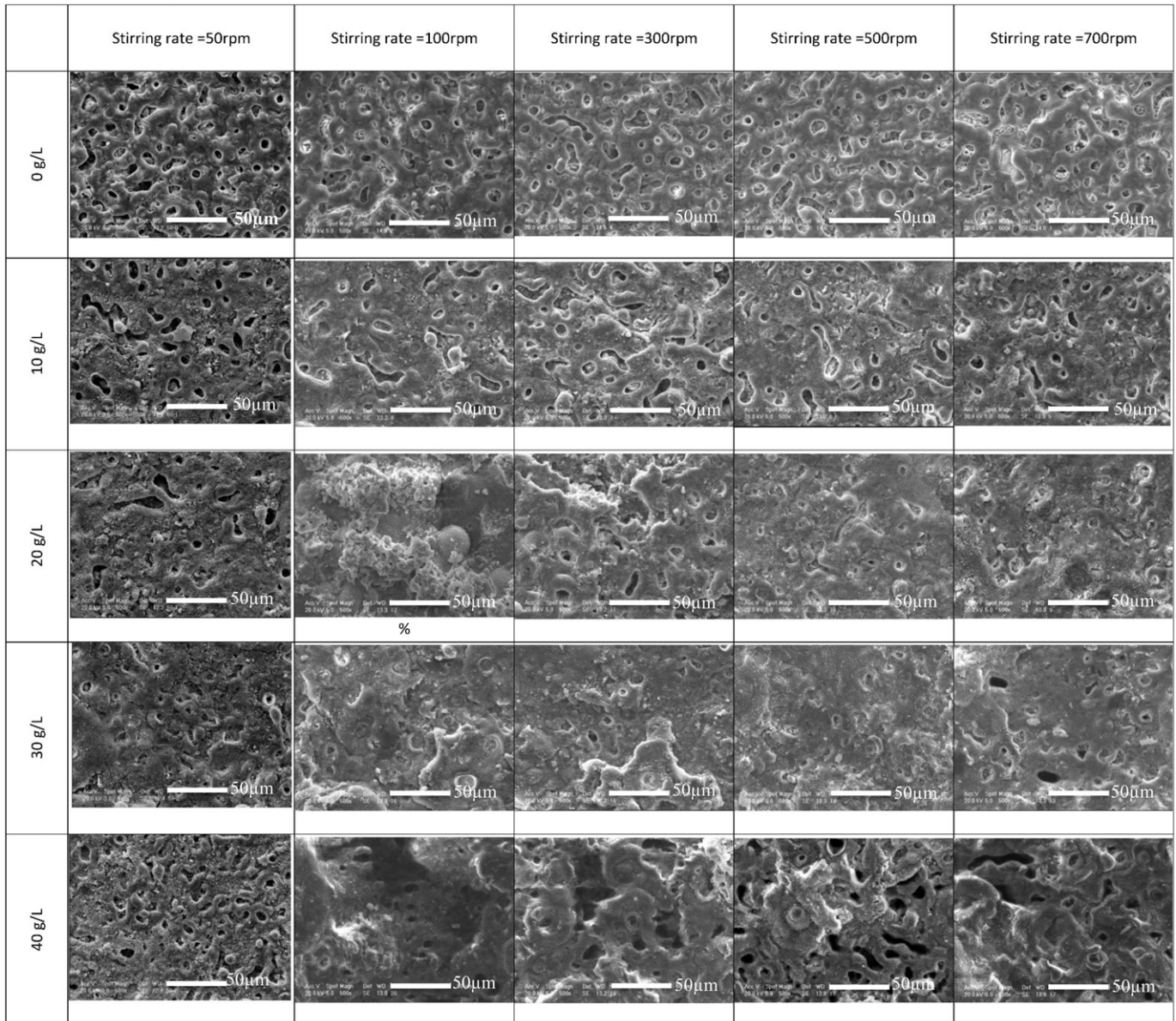


Fig. 3. SEM images of coated samples at different alumina concentration and different stirring rates.

nanoparticles in the electrolyte, at all stirring rates, firstly, the concentration of nanoparticles in the coating is increased up to 30 g/L, and then it reaches a constant value. This constant value can be considered as the saturation limit such that nanoparticles cannot be absorbed any more at higher levels. Reaching this value of saturation may be caused by the saturation of the nanoparticle absorption sites. In PEO coating, the preferred sites of nanoparticles' absorption in the coating are stressful coating sites such as cracks or micro-cracks [24]. These nanoparticles fill the structural defects and porosity. By filling these preferential sites of nanoparticles, the site selection factor of coating is reduced, and nanoparticle absorption in the coating reaches a saturation value. Another reason that has been reported in the literature is agglomeration of nanoparticles at high concentrations that leads to reaching a saturation point of the presence of nanoparticles in the coating [31]. One more factor can be the effect of electrolyte stirring rate on the absorption of nanoparticles. As it can be observed under a fixed nanoparticles concentration in the electrolyte (Fig. 2), the highest absorption of nanoparticles has occurred at a rate of 100 rpm, and at lower stirring rate (50 rpm) the strength of stirring is not enough for absorption of high amount of alumina nanoparticle; thus at this stirring rate, low amount of nanoparticle was absorbed in the PEO coating. By increasing the

electrolyte stirring rate, the nanoparticles' absorption level is decreases, so that the lowest absorption of nanoparticles occurs at the highest electrolyte stirring rate. Reduced concentration of nanoparticles at higher stirring rates can be due to collision factor [32] such that at higher stirring rates, alumina nanoparticles are removed from the anode surface due to high turbulence, and the amount of nanoparticles absorption in the coating is reduced. Also, based on the Foster model [33], by increasing the stirring rate, the force applied on the nanoparticles on the electrode surface increases; this, in turn, reduces the nanoparticles absorption at higher stirring rate.

3.2. Morphology, composition and porosity

Electrolyte composition and presence of various particles in the electrolyte and their absorption in the coating have a significant effect on the morphology and porosity of the coating [34]. Surface and cross-sectional SEM images of the coated specimens at different concentrations of alumina nanoparticles in the electrolyte, and different stirring rates are presented in Figs. 3 and 4, respectively. As clearly shown in the figures, there are pancake-shaped structures in most of the figures with different pores; these pancakes are evenly distributed across the entire

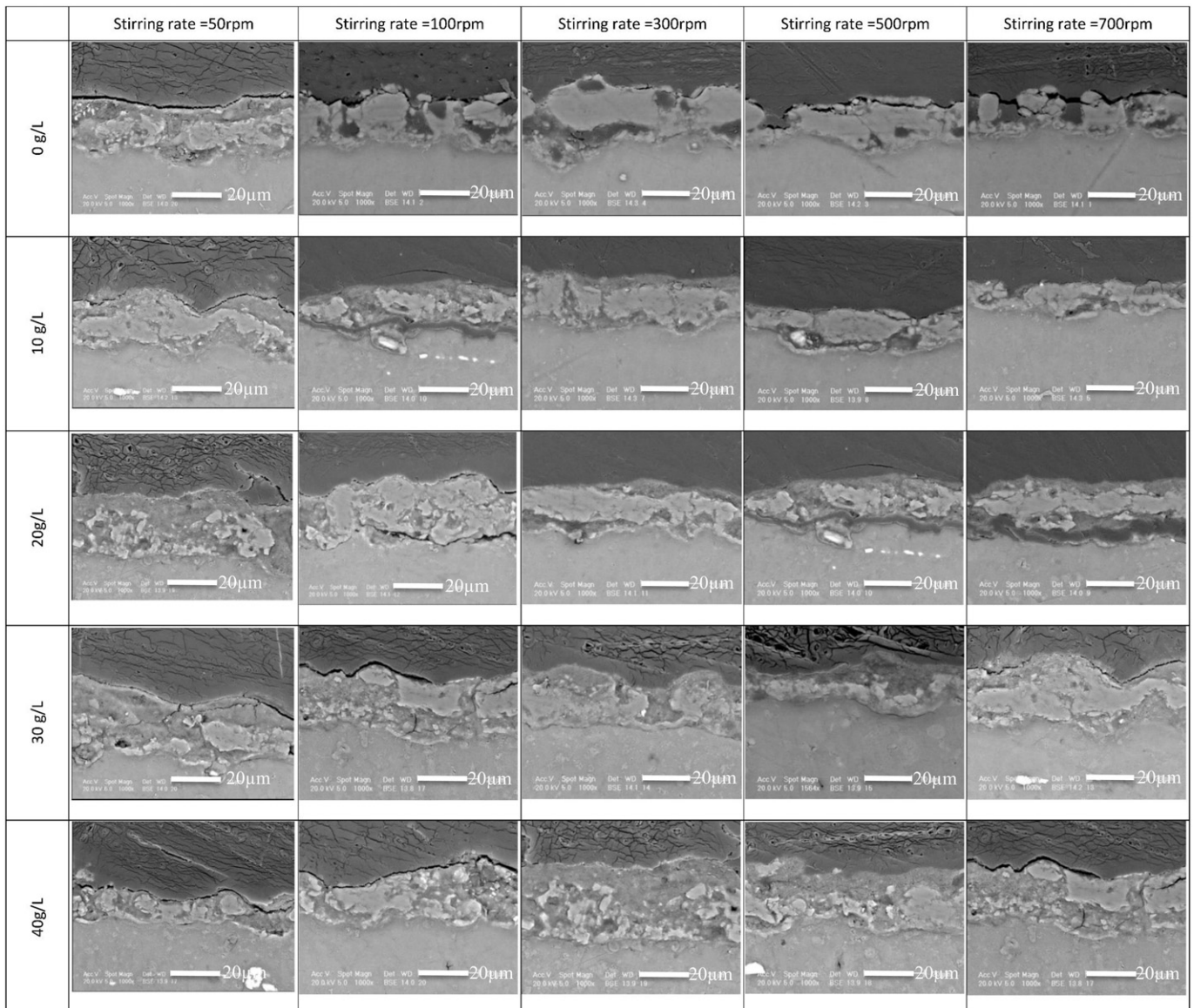


Fig. 4. Cross sectional SEM images of coated samples at different alumina concentration and different stirring rates.

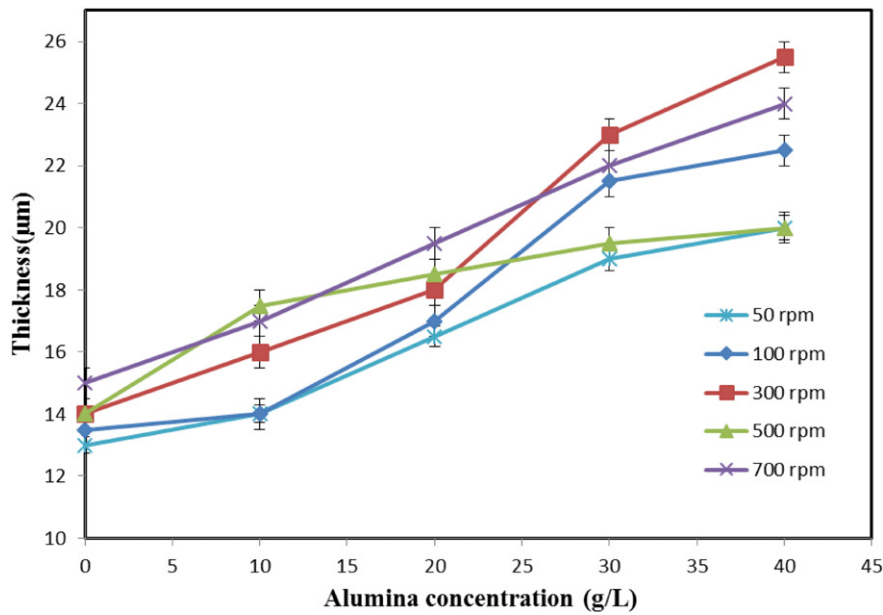


Fig. 5. Coating thickness variation curves as a function of stirring rate of electrolyte and the concentration of nanoparticles in the electrolyte.

surface. Also in some specimens, the pores of the surface are completely closed. It is believed that the formation of these pancake-shaped structure and micro-pores on the coating is due to the formation of discharge channels on the coating surface. The discharges or micro-sparks can impose high pressure and temperature on the surface by high energy, which melts the material in the discharge area, and the molten is rapidly frozen when faced by the cold electrolyte, also a pancake structure is formed with a micro pore at the center of each pancake and discharge is made within that micro-pore [35,36]. As presented in Fig. 3, at a constant stirring rate, by increasing the concentration of nanoparticles in the electrolyte, most of the pores on the surface are closed, and the

porosity is reduced. Generally, it is believed that nanoparticles penetrate into and fill the pores [37,38], this filling improves other properties such as corrosion resistance of the coating (that is discussed in the later sections). Sarbishei et al. [39] analyzed the effect of alumina nanoparticles on the morphology and the amount of porosity, and concluded that by increasing the percentage of nanoparticles in the electrolyte, the percentage of surface porosity decreases. Furthermore, at very high stirring rates, and high concentrations of nanoparticles in the electrolyte, the percentage of surface porosity is high due to desorption of nanoparticles from the electrode surface because of high tolerance flow. The reason for of high porosity of the fabricated coating at 50 rpm is low absorption

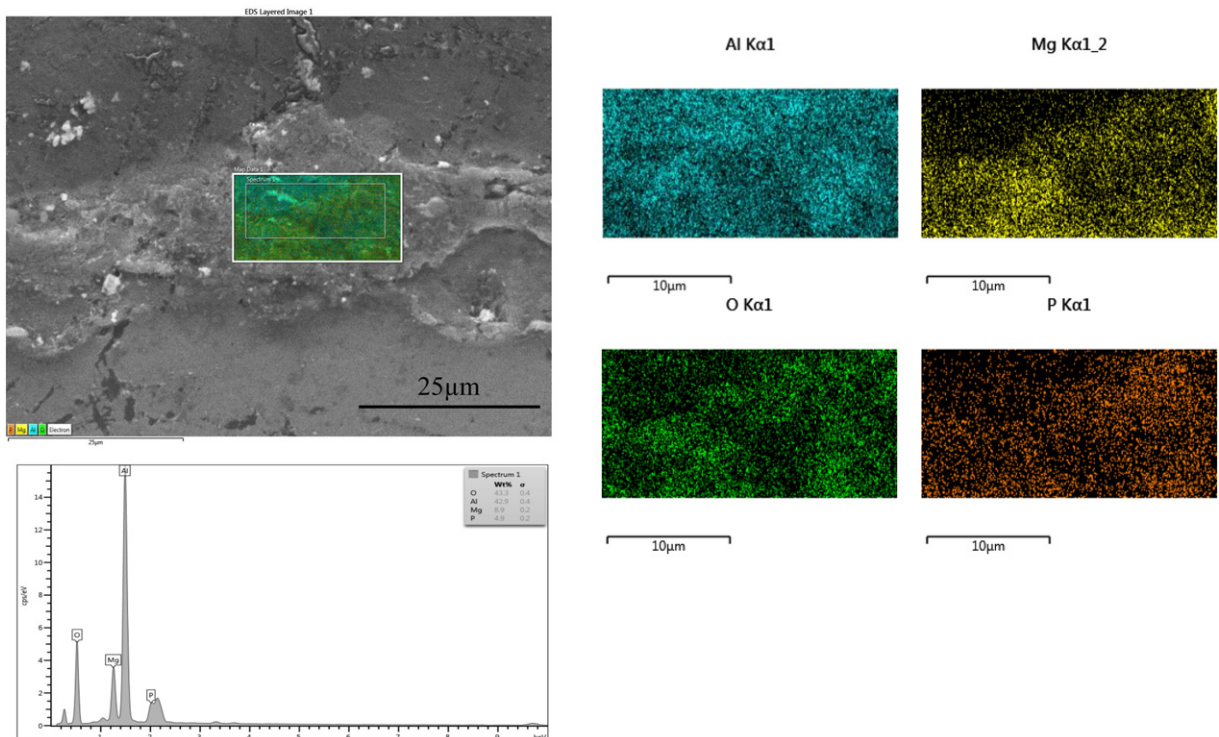


Fig. 6. EDS analysis and elemental mapping of sample coated at 100 rpm and 30 g/L alumina nanoparticle.

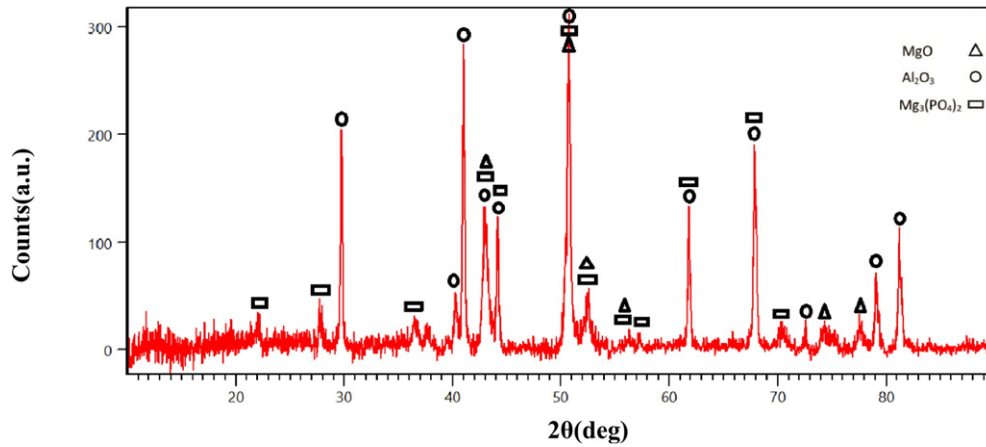


Fig. 7. XRD pattern of sample coated at 100 rpm and 30 g/L alumina nanoparticle.

of alumina nanoparticle in this stirring rate due to low stirring strength. Another reason of high surface porosity of the coating at 500 and 700 rpm and of 40 g/L concentration of alumina nanoparticles is the synergic effect of the possibility of agglomeration at high concentrations of nanoparticles in the electrolyte and high tolerance flow of the electrolyte at high stirring rates. In such conditions, absorption of nanoparticles into the pores decreases and surface porosity increases significantly.

The cross-sectional images of the coatings are also shown in Fig. 4. It is observed that in most cases, there is a good cohesion and adhesion between the coating and the substrate. In most situations, the thickness is between 15 and 25 μm . Coating thickness variation curves as a function of the stirring rate of the electrolyte and the concentration of nanoparticles in the electrolyte are shown in Fig. 5. By increasing the concentration of nanoparticles in the electrolyte, the coating thickness increases up to 30 g/L in all stirring rates and then it reaches to a constant value. These data are in accordance with the data of coating weight variations. But an important difference observed in the data regarding weight gain and increased thickness of the coating is the impact of stirring rate. The stirring rate has no significant impact on the thickness of the coating has also little effect on the thickness of the coating; however, as mentioned

before, by increasing the stirring rate, the weights gain of the coating decrease. Thus, by considering the approximate constant thickness of coating as a result of changes in the electrolyte stirring rate, it can be concluded that the coating porosity is lower at lower stirring rates, which is a reason for the higher absorption of nanoparticles at lower electrolyte stirring rates.

So far, it is concluded that the lowest coating porosity and the highest coating absorption are in the electrolyte containing 30 g/L of alumina nanoparticles and in the electrolyte stirring rate of 100 rpm. Thus this coating was selected to analyze the coating composition. EDS analysis from the cross-section of fabricated coating at this stirring rate is represented in Fig. 6, it is seen, the major elements in the coating are Mg, Al, P and O. Mg is originated from phases that formed during the PEO process, and P is originated from the used phosphate base electrolyte. The source of Al is absorption of alumina nanoparticle from the electrolyte into the coating. Also it is seen from the elemental mapping, that all elements are distributed uniformly across the coating. X-ray diffraction (XRD) spectrum for this specimen is shown in Fig. 7. Some peaks of MgO, Al₂O₃ and Mg₃(PO₄)₂ are marked in the XRD pattern. MgO peak is associated with the created oxide layer formed on the

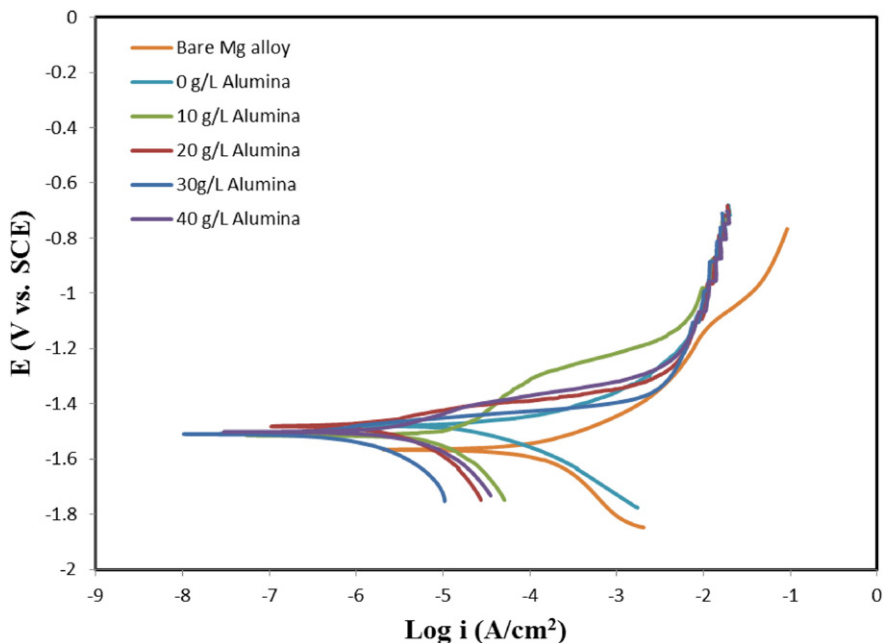


Fig. 8. Potentiodynamic polarization curves of samples coated in electrolytes with different alumina nanoparticle concentration.

Table 1
Results of polarization test for samples coated at different alumina concentration.

Alumina concentration (g/L)	β_a (mv/decade)	β_c (mv/decade)	i_{corr} ($\mu\text{A}/\text{cm}^2$)	R_p (kohm·cm ²)	Corr rate (mpy)	E (mV vs. SCE)
0	298.801	151.626	18.89172	2.314899	7.423	–1561
10	196.708	195.401	12.35414	3.449861	8.81	–1529
20	112.951	44.055	2.179618	6.322093	1.981	–1478
30	63.64	35.849	0.652102	15.28934	0.5924	–1509
40	112.523	89.572	2.791083	7.768863	2.536	–1500
Bare Mg alloy	113.473	65.727	31.01911	0.583366	28.17	–1483

substrate during the process. Since in PEO process, substrate is considered as the anode, under strong electric field, Mg dissolution is based on reaction 1, and magnesium ions are formed.



Oxide film formation on Mg is due to the outward penetration of the formed magnesium ions and the inward penetration of oxygen and phosphate ions in the electrolyte. In such conditions, the reactions 2 and 3 lead to the formation of magnesium oxide and magnesium phosphate respectively [40]:



Alumina peak is related to the alumina nanoparticles existing in the coating, and due to their high concentrations in the electrolyte and coating, their amount is also high in the XRD pattern. Apart from the peaks associated with magnesium oxide and alumina, there are peaks in the XRD pattern the formation of which is based on reaction 3; and since its level is low in the coating, it presents low and weak peaks in the XRD pattern. It is noteworthy to say that MgO and Mg₃(PO₄)₂ phases are caused by the reactions between the ions originating from the substrate as well as the electrolyte ions. Thus the presence of these peaks in the XRD spectrum indicates the reaction between electrolyte and substrate, and also their participation in the coating formation process.

3.3. Corrosion resistance

3.3.1. Potentiodynamic polarization

As mentioned previously, the highest nanoparticle absorption occurred at the electrolyte stirring rate of 100 rpm; thus to study the corrosion resistance, this electrolyte stirring rate (100 rpm) was considered, and the effect of different concentrations of nanoparticles at this stirring rate on corrosion resistance was studied. The polarization curves of the coated specimens in different concentrations of alumina nanoparticles are shown in Fig. 8. Corrosion current density, corrosion potential and polarization resistance are important parameters in evaluation of corrosion behavior. The results of calculation of corrosion current density, polarization resistance and corrosion potential of polarization curves are shown in Table 1. By comparing the uncoated specimens and the specimens coated at different concentrations of nanoparticles, it can be concluded that the corrosion resistance of the substrate is improved by applying the coating. It is also observed that the corrosion potential of the coated specimens is more positive than that of the uncoated specimen that means less corrosion tendency of the coated samples [41]. Improved corrosion resistance due to adding nanoparticles to the electrolyte and absorption of nanoparticles in the coating has also been reported by other researchers [42]. It can be noted that by increasing the concentration of nanoparticles in the electrolyte up to 30 g/L, the corrosion current density decreases; however, it increases in the specimen coated in 40 g/L. The oxide film formed on the surface increases the corrosion resistance of the metal surface by limiting the corrosive ions penetration and reducing the transmission of the ions in the metal-electrolyte interface. The corrosion resistance is influenced by the characteristics of the oxide film such as oxide layer

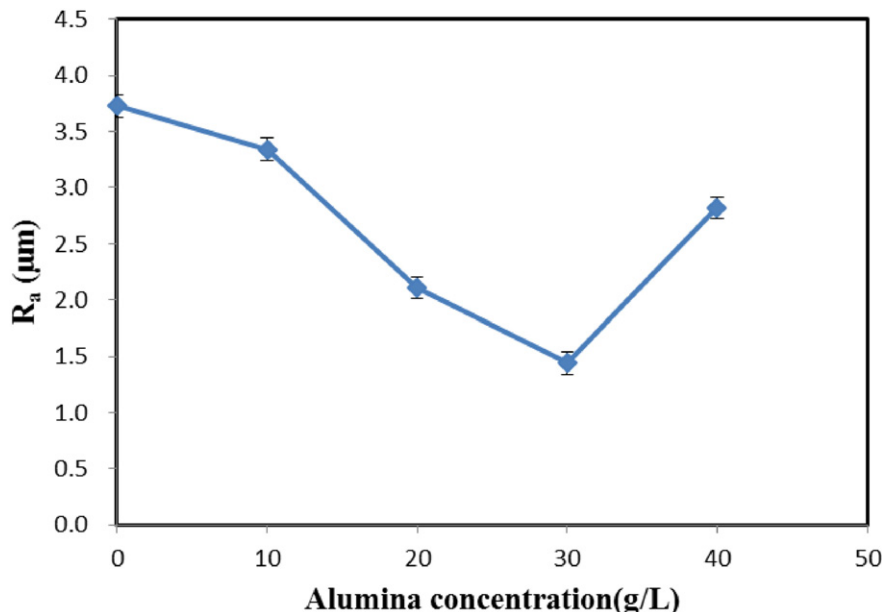


Fig. 9. Variation of R_a as a function of alumina nanoparticle concentration in electrolyte.

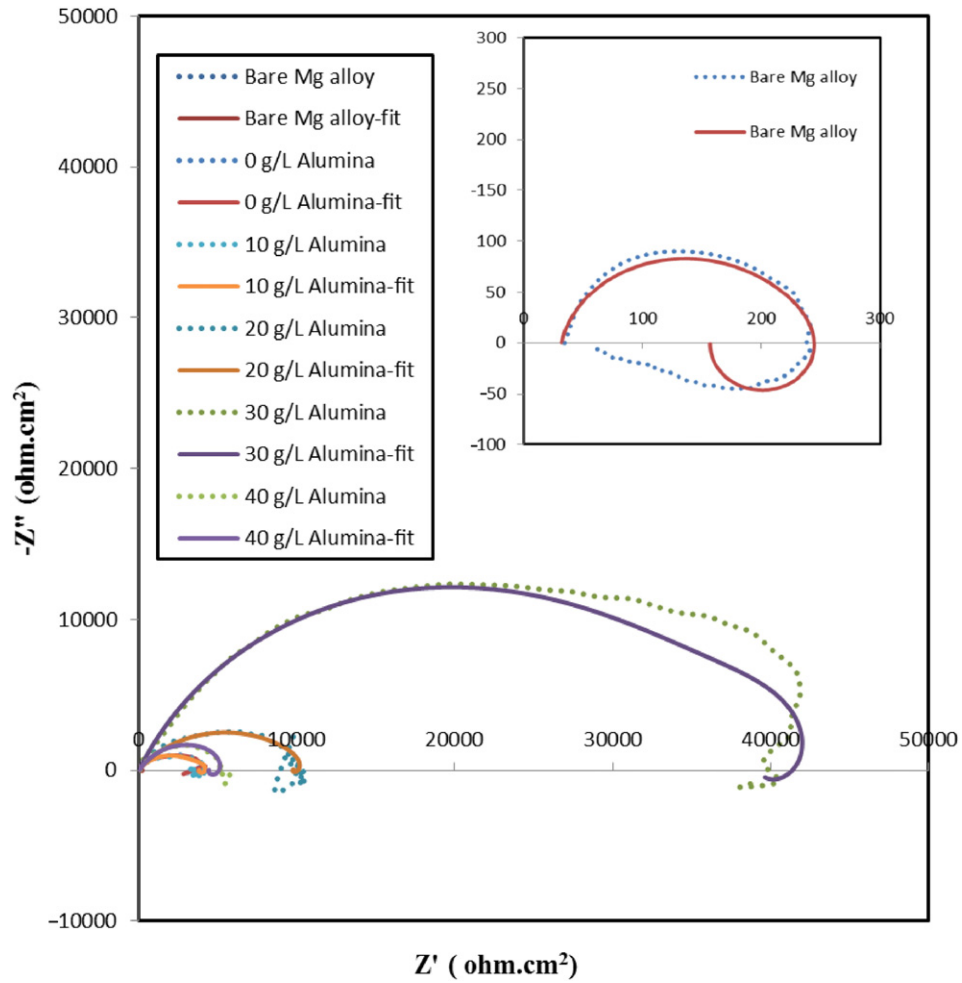


Fig. 10. Nyquist curves of samples coated in electrolytes with different alumina nanoparticle concentration.

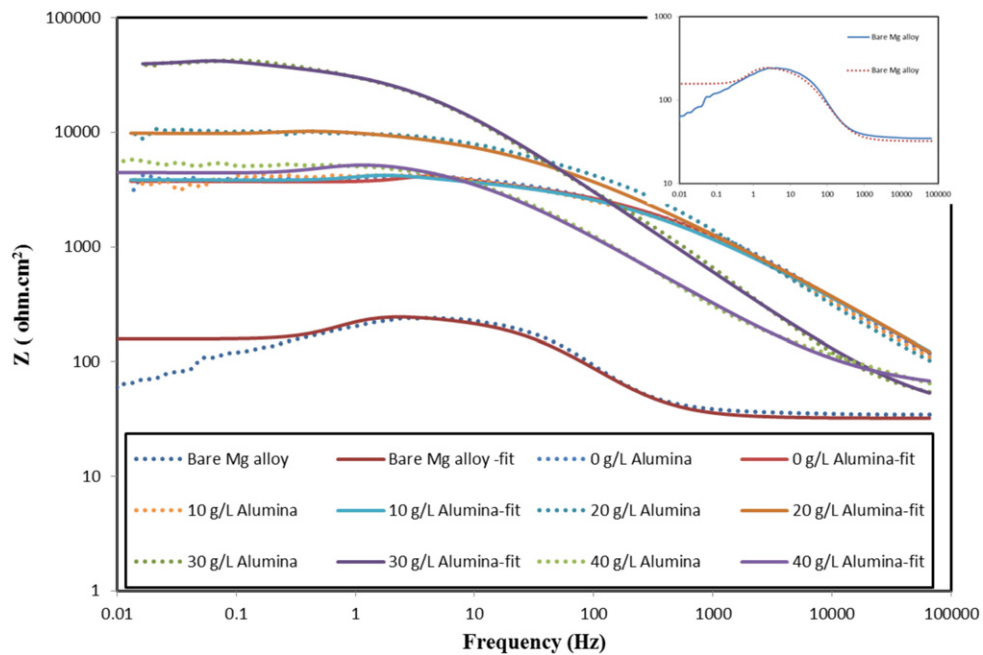


Fig. 11. Bode curves of samples coated in electrolytes with different alumina nanoparticle concentration.

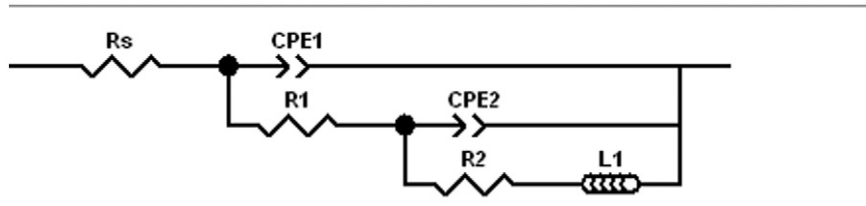


Fig. 12. Equivalent circuit fitted for evaluation of EIS data.

composition, thickness and flaws in the structure, and composition of the corrosive environments. As stated in the nanoparticles absorption section, by increasing the concentration of nanoparticles in the electrolyte, their absorption in the coating increases to 30 g/L, and then reaches a constant value. These nanoparticles reduce the possible entrance routes of corrosive ions to the surface (such as micro-pores and micro-cracks); this prevents the entrance of corrosive ions to the substrate and increases corrosion resistance. It is obvious in the SEM images that by increasing the concentration of nanoparticles in the electrolyte and thus increasing their absorption, many coating pores are closed, and the corrosion resistance increases.

Another factor affecting the corrosion resistance of coating is the surface roughness. It is, generally, accepted that the rougher surface is more susceptible to corrosion. The amount surface roughness curve as a function of the concentration of alumina nanoparticles is shown in Fig. 9. It is observed that by increasing the concentration of nanoparticles in the electrolyte to 30 g/L and higher absorption of nanoparticles, surface roughness is reduced; however, it increases at the level of 40 g/L. The reason for reduced surface roughness at 30 g/L is the filling of surface pores by the nanoparticles, which improves the corrosion resistance as well.

3.3.2. Electrochemical impedance spectroscopy

To further study the corrosion behavior of the coatings fabricated in different concentrations of alumina nanoparticles and also confirming the results of potentiodynamic polarization, accurate electrochemical impedance spectroscopy studies were performed on the specimens. The studies were conducted on solution NaCl 3.5 wt% at room temperature. The Nyquist curves and the Bode curves of different specimens are shown in Figs. 10 and 11 respectively. As can be seen, by increasing the concentration of nanoparticles in the electrolyte, the diameter of the Nyquist curves, which indicate polarization resistance, are increased up to 30 g/L, then it is decreased at the concentration of 40 g/L. So it can be concluded that the corrosion resistance of the coating is increased to a concentration of 30 g/L and then it is decreased. There is a good relationship between the polarization curves and the Nyquist curves' data. Also in the Bode curves, the highest value of total impedance at low frequencies, which represents the overall resistance of the coating, is observed at a concentration of 30 g/L; this confirms the highest corrosion resistance of these specimens.

To estimate the parameters associated with EIS, an equivalent circuit was fitted for the data (Fig. 12). The parameters relating to EIS are also shown in Table 2; there are two constants phase elements in the equivalent circuit: the first constant phase element in the lower range is associated with the formation of dense layer in the anodizing process, and

the second constant phase element in the range of high frequencies is associated with the porous layer. In the equivalent fitted circuit, R_s represents solution resistance, R_1 is porous layer resistance, CPE_1 denotes a constant phase element of porous layer, R_2 represents dense layer resistance and CPE_2 is constant phase element of dense layer. In this study, the constant phase element has been used instead of pure capacitor due to the heterogeneous factor of the surface [43,44]. The impedance element of constant phase is defined as follows:

$$Z_{CPE} = \frac{1}{T(j\omega)^n} \quad (4)$$

where, T is the admittance constant, j denotes imaginary unit, ω indicates angular frequency, and n is the experimental power CPE, which varies between 0 and 1. 0 and 1 values of n indicate pure resistance and pure capacitance. In the Nyquist curves, an inductive loop is also observed at lower frequencies range that are also presented in the equivalent circuit. The presence of induction loop in the uncoated magnesium specimen is consistent with previous studies; the reason of is the dissolution of the substrate and the porosity of magnesium substrate [45,46]. Similar behavior is also observed in the coated specimens. In general, PEO coatings include a porous outer layer and a porous inner layer. The presence of induction loop in the coated specimens within the low frequency range indicates pitting corrosion during the electrochemical testing, which is because of the porous layer [46,47]. The existence of pores on the surface causes the heterogeneity of the surface and a path for the entrance of the corrosive ions to the substrate; as mentioned before, when the concentration of nanoparticles in the electrolyte increases, the nanoparticles are placed in the pores to fill these pores and make the surface homogeneous and uniform. The homogeneity of the surface in the impedance curve data appears in "n", and as this value is closer to 1, the surface becomes more homogenous. As shown in the data, the highest value of "n" among the coated specimens is associated with the specimen formed in the electrolyte containing 30 g/L; so it can be expected that the most homogeneous surface is associated with these specimens. This homogeneity is associated with the filling of the pores by nanoparticles. So it can be concluded that the highest corrosion resistance is associated with these specimens.

3.4. Wear behavior

To study the wear behavior of the coated specimens, the abrasion pin on disk test was used. The sliding distance for all specimens is the same and equals 200 m. The abrasion tests were conducted on the specimens with the concentrations ranging from 0 to 40 g/L of alumina

Table 2
EIS fitted results for samples coated at different alumina concentration.

Alumina concentration (g/L)	R_s (ohm·cm ²)	n_2	COE_2 (ohm ⁻¹ ·cm ⁻²)	R_2 (ohm·cm ²)	n_1	CPE_1 (ohm ⁻¹ ·cm ⁻²)	R_1 (ohm·cm ²)
Bare Mg alloy	32		4.26×10^{-6}	120	0.89	7.7×10^{-3}	5
0	30	0.36	2.9×10^{-6}	3500	0.62	3.5×10^{-4}	250
10	32	0.28	3.8×10^{-6}	3627	0.6	6.3×10^{-4}	239.5
20	34	0.1	5.7×10^{-6}	9900	0.55	7×10^{-4}	50
30	34.3	0.32	3.03×10^{-6}	35,000	0.72	1.5×10^{-4}	5500
40	35	0.013	1.2×10^{-5}	4184	0.65	5×10^{-4}	265

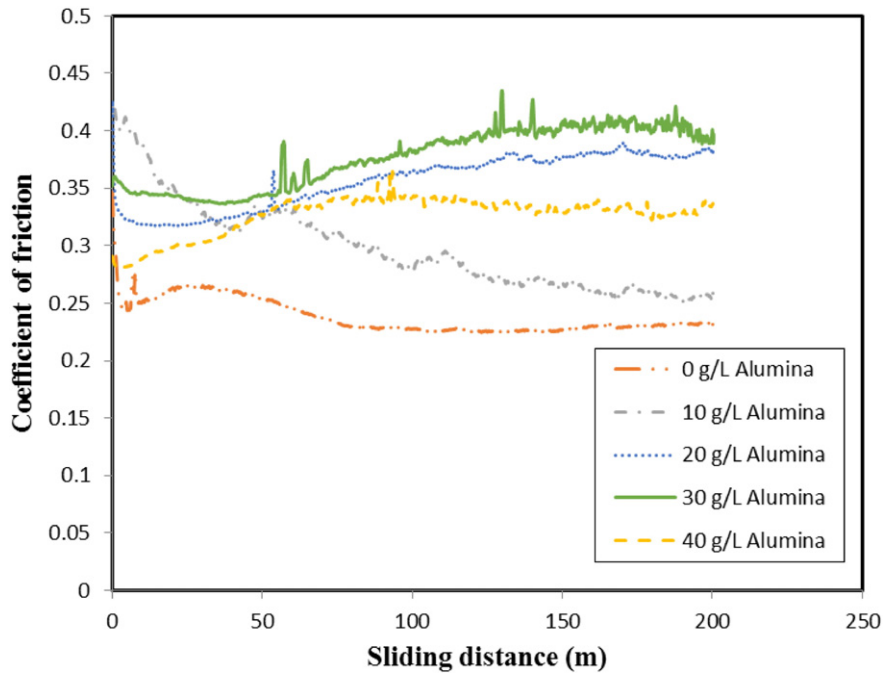


Fig. 13. Variation of Friction coefficient of samples coated at different conditions.

nanoparticles with the electrolyte stirring rate of 100 rpm. The Variations of friction coefficient of different samples are shown in Fig. 13. In most cases, the wear process is regular; however, it is not regular in the specimens without nanoparticles. During the wear test process, we observed that the coating is fragmented and detached during testing due to the poor areas and pores inside the coating, making the coating non-uniform, proper areas for nucleation, and cracking in the coating and their detachment. As illustrated in the SEM images in Fig. 3, the proper areas are the pores without nanoparticles and the presence of porosity in the coating or cracks at the interface of the coating and the substrate. Yu et al. [48]; who studied improvement in the wear resistance of the alloys at the presence of SiC nanoparticles, also reported poor areas in the coating as the reason for the cracking and detachment of the coating. The wear rate curve as a function of alumina nanoparticle concentration is represented in Fig. 14. The wear rate curve suggests that the specimens with alumina nanoparticles have lower wear rate than those without nanoparticles due to filling of the PEO porous

pores; the amount of filling varies with different concentrations [49] and confirmed by Gheyfani et al. [14,16]. In most studies, adding nanoparticles increased abrasion resistance [50]. As seen in the sample wear test graph, for the specimens with the concentration of 30, 20 and 40 g/L of alumina nanoparticle, the friction coefficient versus sliding distance is upward but the curves of the sample 10 and 0 g/L alumina nanoparticle friction coefficient is downward. For the specimen with the concentration of 30 g/L, the friction coefficient starts with 0.36, and after a short drop, it starts to increase; and after reaching a maximum coefficient, it is stabilized at the friction coefficient of 0.38. In the specimen with the concentration of 20 g/L, the friction coefficient curve in terms of distance starts with 0.34, and after a similar trend, it is stabilized at the friction coefficient of 0.38. The curve of 40 g/L has the same process with the difference that the coefficient of friction after a sudden and severe drop at the beginning of the test starts increasing from 0.28 and reaches the final constant friction coefficient level of 0.42. In the curve of 10 g/L of alumina nanoparticles, the trend of changes in the friction coefficient

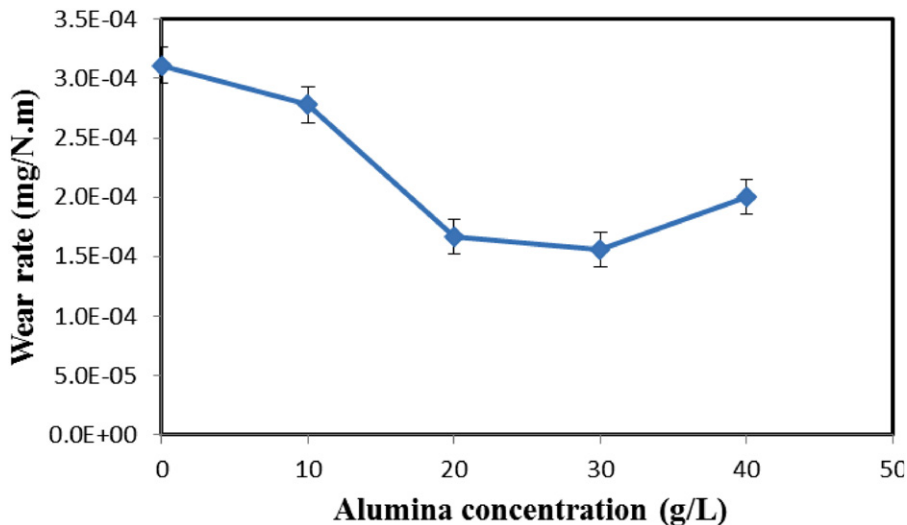


Fig. 14. Wear rate curve as a function of alumina nanoparticle concentration in the electrolyte.

level is downward until it has reaches an almost fixed level; this curve starts with the friction coefficient of 0.42 and ends with the friction coefficient of 0.26. In the specimen without nanoparticles, after almost 50 m, the friction coefficient reaches 0.24; this amount is not changed until the end of the process. In the description of the five curves, it can be mentioned that the sudden drop of friction of coefficient in 30, 40 and 20 g/L concentration of alumina is associated with the accumulation of alumina nanoparticles in the coating at the end of reaction and their failure to be absorbed by the coating; however, the constant increase of the friction coefficient by increasing the distance might be due to the fact that the nanoparticles are absorbed in the pores and the substrate oxide, and by the passage of time and distance, these nanoparticles are in contact with the pin; this increases the friction coefficient and reduces the abrasion. The related interpretations are presented in SEM images in Fig. 3. It means that alumina nanoparticles in the pores and magnesium oxide are clearly visible, implying that the nanoparticles are uniformly distributed in the coating [51]. Regarding the downward trend of curve 10, it can be noted that the amount of nanoparticles is too low to increase the wear resistance and prevent the abrasion of the coating, which is fixed after 125 m. Fluctuations in the friction coefficient are observed in all of these curves, probably due to the fine pieces of the coating that are removed from the surface and are in contact with the pin [48]. The changes in the wear rate are presented as a function of the concentration of nanoparticles (Fig. 13), indicating that the lowest wear rate is at the concentration of 30 g/L, and the amount of coating loss is minimum. After that, the lowest wear rates are associated with 20, 40, 10 and 0 g/L specimens these amount of changes indicated that by increasing the absorption of nanoparticles, the wear rate is decreased [52,53]

4. Conclusions

In this study, the effect of electrolyte stirring rate and concentration of alumina nanoparticles in the electrolyte on the absorption of nanoparticles in the coating fabricated by plasma electrolytic oxidation on magnesium was investigated. The maximum amount of absorption of nanoparticles was obtained at the stirring rate of 100 rpm. The results showed that, at higher stirring rates, due to high turbulent current and washing of nanoparticles from the anode surface, the nanoparticles' absorption level is decreased. Also, by increasing the concentration of alumina nanoparticles in the electrolyte to 30 g/L, their absorption in the coating is increased and then reaches saturated level. Furthermore, high absorption of nanoparticles and decreased amount of porosity in the coating at 100 rpm and 30 g/L concentration of nanoparticles lead to the best corrosion resistance in the coating. The wear behavior studies indicated that the lowest wear rate is associated with the electrolyte containing 30 g/L alumina nanoparticles.

References

- [1] C.S. Roberts, *Magnesium and its Alloys*, Wiley, 1960.
- [2] M.M. Avedesian, H. Baker, *ASM Speciality Handbook: Magnesium and Magnesium Alloys*, Vol. 27, New York: ASM International, 1999.
- [3] K.U. Kainer, F. Kaiser, *Magnesium Alloys and Technology*, 2003.
- [4] G.-L. Song, *Corrosion of Magnesium Alloys*, Elsevier, 2011.
- [5] R.W. Revie, H.H. Uhlig, *Uhlig's Corrosion Handbook*, John Wiley & Sons, 2011.
- [6] Z.A.X.Y.Q. Yufeng, W.Z.H.Y.C. Ying, Chemical surface treatment for magnesium alloys [J], *Corr. Protection* 2 (2000) 002.
- [7] K. De Long Herbert, *Surface Treatment of Magnesium Alloys* Google Patents 1947.
- [8] R. Arrabal, E. Matykina, T. Hashimoto, P. Skeldon, G. Thompson, Characterization of AC PEO coatings on magnesium alloys, *Surf. Coat. Technol.* 203 (2009) 2207–2220.
- [9] M. Aliofkhaezai, A.S. Rouhaghdam, P. Gupta, Nano-fabrication by cathodic plasma electrolysis, *Crit. Rev. Solid State Mater. Sciences* 36 (2011) 174–190.
- [10] J. Cai, F. Cao, L. Chang, J. Zheng, J. Zhang, C. Cao, The preparation and corrosion behaviors of MAO coating on AZ91D with rare earth conversion precursor film, *Appl. Surf. Sci.* 257 (2011) 3804–3811.
- [11] X. Lu, C. Blawert, M.L. Zheludkevich, K.U. Kainer, Insights into plasma electrolytic oxidation treatment with particle addition, *Corros. Sci.* 101 (2015) 201–207.
- [12] A. Michaelis, Valve metal, Si and ceramic oxides as dielectric films for passive and active electronic devices, *Adv. Electrochem. Sci. Eng.* 10 (2008) 1–106.
- [13] G.-H. Lv, H. Chen, L. Li, E.-W. Niu, H. Pang, B. Zou, S.-Z. Yang, Investigation of plasma electrolytic oxidation process on AZ91D magnesium alloy, *Curr. Appl. Phys.* 9 (2009) 126–130.
- [14] M. Gheyhani, H. Bagheri, H. Masiha, M. Aliofkhaezai, A. Sabour Rouhaghdam, T. Shahrabi, Effect of SMAT preprocessing on MAO fabricated nanocomposite coating, *Surf. Eng.* 30 (2014) 244–255.
- [15] M. Aliofkhaezai, R.S. Gharabagh, M. Teimouri, M. Ahmadzadeh, G.B. Darband, H. Hasannejad, Ceria embedded nanocomposite coating fabricated by plasma electrolytic oxidation on titanium, *J. Alloys Compd.* 685 (2016) 376–383.
- [16] M. Gheyhani, M. Aliofkhaezai, H. Bagheri, H. Masiha, A.S. Rouhaghdam, Wettability and corrosion of alumina embedded nanocomposite MAO coating on nanocrystalline AZ31B magnesium alloy, *J. Alloys Compd.* 649 (2015) 666–673.
- [17] C. Dunleavy, I. Golosnoy, J. Curran, T. Clyne, Characterisation of discharge events during plasma electrolytic oxidation, *Surf. Coat. Technol.* 203 (2009) 3410–3419.
- [18] H. Sharifi, M. Aliofkhaezai, G.B. Darband, A.S. Rouhaghdam, Tribological properties of PEO nanocomposite coatings on titanium formed in electrolyte containing ketoconazole, *Tribol. Int.* 102 (2016) 463–471.
- [19] H. Sharifi, M. Aliofkhaezai, G.B. Darband, A.S. Rouhaghdam, Characterization of PEO nanocomposite coatings on titanium formed in electrolyte containing atenolol, *Surf. Coat. Technol.* 304 (2016) 438–449.
- [20] R. Hussein, D. Northwood, X. Nie, The effect of processing parameters and substrate composition on the corrosion resistance of plasma electrolytic oxidation (PEO) coated magnesium alloys, *Surf. Coat. Technol.* 237 (2013) 357–368.
- [21] S. Zhongcai, K. Bing, Effect of additive Al₂O₃ powders on micro-arc oxide coating of magnesium alloy, *Sci. Eng. Compos. Mater.* 22 (2015) 497–502.
- [22] J.J. Ulbrecht, G.K. Patterson, *Mixing of Liquids by Mechanical Agitation*, Taylor & Francis, 1985.
- [23] P. Kundu, L. Cohen, *Fluid Mechanics*, 638 pp, Academic, Calif, 1990.
- [24] T.S. Lim, H.S. Ryu, S.-H. Hong, Electrochemical corrosion properties of CeO₂-containing coatings on AZ31 magnesium alloys prepared by plasma electrolytic oxidation, *Corros. Sci.* 62 (2012) 104–111.
- [25] S. Di, Y. Guo, H. Lv, J. Yu, Z. Li, Microstructure and properties of rare earth CeO₂-doped TiO₂ nanostructured composite coatings through micro-arc oxidation, *Ceram. Int.* 41 (2015) 6178–6186.
- [26] S. Sarbishei, M.A.F. Sani, M.R. Mohammadi, Study plasma electrolytic oxidation process and characterization of coatings formed in an alumina nanoparticle suspension, *Vacuum* 108 (2014) 12–19.
- [27] M. Shokouhfar, S. Allahkaram, Formation mechanism and surface characterization of ceramic composite coatings on pure titanium prepared by micro-arc oxidation in electrolytes containing nanoparticles, *Surf. Coat. Technol.* 291 (2016) 396–405.
- [28] X. Lu, C. Blawert, Y. Huang, H. Ovri, M.L. Zheludkevich, K.U. Kainer, Plasma electrolytic oxidation coatings on Mg alloy with addition of SiO₂ particles, *Electrochim. Acta* 187 (2016) 20–33.
- [29] K.R. Shin, Y.G. Ko, D.H. Shin, Surface characteristics of ZrO₂-containing oxide layer in titanium by plasma electrolytic oxidation in K₄P₂O₇ electrolyte, *J. Alloys Compd.* 536 (2012) S226–S230.
- [30] M. Aliofkhaezai, A.S. Rouhaghdam, T. Shahrabi, Abrasive wear behaviour of Si₃N₄/TiO₂ nanocomposite coatings fabricated by plasma electrolytic oxidation, *Surf. Coat. Technol.* 205 (2010) S41–S46.
- [31] M. Aliofkhaezai, A.S. Rouhaghdam, E. Ghobadi, Characterization of Si₃N₄/TiO₂ nanocomposite coatings prepared via micro arc oxidation, *J. Nanosci. Nanotechnol.* 11 (2011) 9057–9060.
- [32] S. Yeh, C. Wan, A study of SiC/Ni composite plating in the Watts bath, *Plat. Surf. Finish.* 84 (1997) 54–58.
- [33] J. Foster, B. Cameron, Effect of current density and agitation on the formation of electrodeposited composite coatings, *Trans. Inst. Met. Finish.* 54 (4) (Winter 1976) 178–183 (1976).
- [34] W. Kai, K. Bon-Heun, L. Chan-Gyu, K. Young-Joo, L. Sung-Hun, B. Eungsun, Effects of electrolytes variation on formation of oxide layers of 6061 Al alloys by plasma electrolytic oxidation, *Trans. Nonferrous Metals Soc. China* 19 (2009) 866–870.
- [35] A. Yerokhin, X. Nie, A. Leyland, A. Matthews, Characterisation of oxide films produced by plasma electrolytic oxidation of a Ti–6Al–4V alloy, *Surf. Coat. Technol.* 130 (2000) 195–206.
- [36] Y.-I. Cheng, X.-Q. Wu, Z.-g. Xue, E. Matykina, P. Skeldon, G. Thompson, Microstructure, corrosion and wear performance of plasma electrolytic oxidation coatings formed on Ti–6Al–4V alloy in silicate-hexametaphosphate electrolyte, *Surf. Coat. Technol.* 217 (2013) 129–139.
- [37] D. Wei, Y. Zhou, D. Jia, Y. Wang, Chemical treatment of TiO₂-based coatings formed by plasma electrolytic oxidation in electrolyte containing nano-HA, calcium salts and phosphates for biomedical applications, *Appl. Surf. Sci.* 254 (2008) 1775–1782.
- [38] S.-y. Wang, N.-c. Si, Y.-p. Xia, L. Li, Influence of nano-SiC on microstructure and property of MAO coating formed on AZ91D magnesium alloy, *Trans. Nonferrous Metals Soc. China* 25 (2015) 1926–1934.
- [39] S. Sarbishei, M.A.F. Sani, M.R. Mohammadi, Effects of alumina nanoparticles concentration on microstructure and corrosion behavior of coatings formed on titanium substrate via PEO process, *Ceram. Int.* 42 (2016) 8789–8797.
- [40] S. Durdu, M. Usta, Characterization and mechanical properties of coatings on magnesium by micro arc oxidation, *Appl. Surf. Sci.* 261 (2012) 774–782.
- [41] M. Shokouhfar, C. Dehghanian, M. Montazeri, A. Baradaran, Preparation of ceramic coating on Ti substrate by plasma electrolytic oxidation in different electrolytes and evaluation of its corrosion resistance: part II, *Appl. Surf. Sci.* 258 (2012) 2416–2423.
- [42] M. Laleh, A.S. Rouhaghdam, T. Shahrabi, A. Shanghi, Effect of alumina sol addition to micro-arc oxidation electrolyte on the properties of MAO coatings formed on magnesium alloy AZ91D, *J. Alloys Compd.* 496 (2010) 548–552.

- [43] G. Brug, A. Van Den Eeden, M. Sluyters-Rehbach, J. Sluyters, The analysis of electrode impedances complicated by the presence of a constant phase element, *J. Electroanal. Chem. Inter. Electrochem.* 176 (1984) 275–295.
- [44] J.-B. Jorcin, M.E. Orazem, N. Pébère, B. Tribollet, CPE analysis by local electrochemical impedance spectroscopy, *Electrochim. Acta* 51 (2006) 1473–1479.
- [45] G. Song, A. Atrens, D.S. John, X. Wu, J. Nairn, The anodic dissolution of magnesium in chloride and sulphate solutions, *Corros. Sci.* 39 (1997) 1981–2004.
- [46] X.-j. Cui, X.-z. Lin, C.-h. Liu, R.-s. Yang, X.-w. Zheng, M. Gong, Fabrication and corrosion resistance of a hydrophobic micro-arc oxidation coating on AZ31 Mg alloy, *Corros. Sci.* 90 (2015) 402–412.
- [47] J. Liang, P.B. Srinivasan, C. Blawert, W. Dietzel, Comparison of electrochemical corrosion behaviour of MgO and ZrO₂ coatings on AM50 magnesium alloy formed by plasma electrolytic oxidation, *Corros. Sci.* 51 (2009) 2483–2492.
- [48] L. Yu, J. Cao, Y. Cheng, An improvement of the wear and corrosion resistances of AZ31 magnesium alloy by plasma electrolytic oxidation in a silicate-hexametaphosphate electrolyte with the suspension of SiC nanoparticles, *Surf. Coat. Technol.* 276 (2015) 266–278.
- [49] H. Li, Y. Sun, J. Zhang, Effect of ZrO₂ particle on the performance of micro-arc oxidation coatings on Ti₆Al₄V, *Appl. Surf. Sci.* 342 (2015) 183–190.
- [50] M. Mohedano, C. Blawert, M. Zheludkevich, Silicate-based Plasma Electrolytic Oxidation (PEO) coatings with incorporated CeO₂ particles on AM50 magnesium alloy, *Mater. Des.* 86 (2015) 735–744.
- [51] Y. Wang, B. Jiang, L. Guo, T. Lei, Tribological behavior of microarc oxidation coatings formed on titanium alloys against steel in dry and solid lubrication sliding, *Appl. Surf. Sci.* 252 (2006) 2989–2998.
- [52] L.R. Krishna, A.S. Purnima, G. Sundararajan, A comparative study of tribological behavior of microarc oxidation and hard-anodized coatings, *Wear* 261 (2006) 1095–1101.
- [53] S.-m. Li, X.-m. Yu, J.-h. Liu, M. Yu, L. Wu, K. Yang, Microstructure and abrasive wear behaviour of anodizing composite films containing SiC nanoparticles on Ti₆Al₄V alloy, *J. Cent. South Univ.* 21 (2014) 4415–4423.